Characteristics Investigation of a Variable Flux Magnetic-Geared Motor Using Mathematical and Numerical Methods

Noboru Niguchi[1], Katsuhiro Hirata[1], Akira Kohara[1], and Kazuaki Takahara[1]

[1]Osaka University, Suita, Osaka, 5650871, Japan, noboru.niguchi@ams.eng.osaka-u.ac.jp

We have studied current superimposition variable flux motors for a traction motor of electric vehicles and electric hybrid vehicles. The power band of the current superimposition variable flux motors was high. However, the torque density was not so high. In this paper, we propose a variable flux magnetic-geared motor in order to increase the torque density of the current superimposition variable flux motors. The N-T characteristics are obtained by mathematical and numerical approaches, and these are compared with each other. Finally, the performance of the variable flux magnetic-geared motor is discussed.

***Index Terms*—Brushless motors, magnetic-geared motor, gears, finite element analysis.**

I. Introduction

We have developed a current superimposition variable flux reluctance motor (CSVFRM) for traction motors of EVs and HEVs [1-2]. This motor have wide power band characteristics compared with conventional motors such as an IPMSM, SRM, and IM. However, the torque density of the CSVFRM was not so high. In this paper, we propose a variable flux magnetic-geared motor (VFMGM) in order to increase the torque density. The N-T characteristics of the VFMGM is calculated by 2 methods: one is a mathematical method using inductances computed by static analyses, the other is a transient electromagnetic field analysis under vector control. Finally, the performance of the VFMGM is discussed.

II. Variable Flux Magnetic-Geared Motor

A. Constitution

A VFMGM in this study is shown in Fig. 1. The VFMGM consists of high- and low-speed rotors, and stator. The high-speed rotor has 10 salient poles, and the low-speed rotor has 22 steel pole pieces. The stator has 12 slots, and where 6-phase concentrated winding coils (A, B, C, D, E, and F) are aligned as shown in Fig. 1.

B. Operational Principle

A 6th-order magnetomotive force is generated in the inner circumference of the stator by applying DC voltages ($+V$ and $-V$) as shown in Fig. 1. The 6th-order magnetomotive force is modulated by a 22th-order permeance due to the low-speed rotor, and 16th- and 28th-modulated harmonics are generated. In addition, the 6th-order magnetomotive force is modulated by the high-speed rotor which has a 10th-order permeance, and 4th- and 16th-order harmonics are generated. The 16th-order harmonics due to the low-speed and high-speed rotors are synchronized. Therefore, the low-speed rotor rotates at a gear ratio of 2.2 (=22/10) when the high-speed rotor is rotated.

In order to synchronize the high-speed rotor with a rotating magnetic field due to the coils, AC voltages are applied to the coils. The 6-phase coils consists of 2 sets of 3-phase coils. Therefore, a 4th-order rotating magnetic field is generated by applying 3-phase AC voltages on the coils. The 4th-order rotating magnetic field due to the coils synchronizes the 4th-order modulated flux due to the magnetomotive force due to the DC voltage and permeance due to the high-speed rotor.

III. Torque-Speed Curve

A. Model

The shape of the VFMGM is shown in Fig. 1, and the specification is shown in TABLE I. In this study, the resistance between the motor and inverter, and iron losses are ignored.

B. Mathematical Method

The torque-speed curve of the VFMGM is mathematically calculated. Similar to a brushless DC motor, the rotation speed and torque are calculated using a flux linkage computed by FEM analysis. However, in the VFMGM, the phase angle difference between the high- and low-speed rotors must be considered.

Fig. 2 shows the flux vector on the d-q coordinate system, where L_d and L_q are the d- and q-axis inductance, respectively, i_d and i_q are the d- and q-axis current, respectively, an ψ_0 and ψ_f are the total flux and flux linkage of the coil, respectively. L_d (= L_q), ψ_0, and ψ_f are computed using a static FEM analysis, and the rotation speed and torque are calculated using (1) and (2).

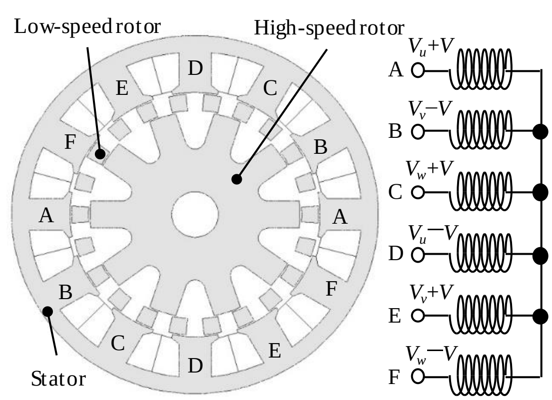

Fig. 1. Variable flux magnetic-geared motor.

$$\begin{pmatrix} v_d \\ v_q \end{pmatrix} = \begin{pmatrix} R_a & 0 \\ 0 & R_a \end{pmatrix}\begin{pmatrix} i_d \\ i_q \end{pmatrix} + \begin{pmatrix} 0 & -\omega L_q \\ \omega L_d & 0 \end{pmatrix}\begin{pmatrix} i_d \\ i_q \end{pmatrix} + \begin{pmatrix} 0 \\ \sqrt{\frac{3}{2}}\omega\psi_f \end{pmatrix} \quad (1)$$

$$T = p_n\left\{\sqrt{\frac{3}{2}}\psi_f i_q + (L_d - L_q) i_d i_q\right\} \quad (2)$$

where v_d and v_q are the d- and q-axis voltage, R_a is the phase resistance, ω is the rotation speed, T is the torque, and p_n is the number of pole pairs.

The phase angle difference between the rotors is defined as a phase angle from a magnetically stable position. The output torque is decided by the phase angle difference. The phase angle difference is changed when a given current is applied, and the phase angle difference where the average torque of the high-speed rotor is zero is searched. When the average torque of the high-speed rotor is zero, the reaction torque from the low-speed rotor and the current torque due to the coil is equal.

The relationship between the phase angle difference and high-speed rotor torque is shown in Fig. 3 when the DC current is 40 A and the AC current amplitude is 12.5 A. The high-speed rotor torque is computed using FEM analysis. From Fig. 3, the average torque of the high-speed rotor is zero when the phase angle difference is 33 deg. Therefore, the inductance and flux linkage when the DC current is 40 A and the AC current amplitude is 12.5 A is obtained by a static analysis which the phase angle difference between the rotors is 33 deg.

In this way, the torque and rotation speed of the high-speed rotor are obtained. In order to convert the torque and rotation speed of the high-speed rotor to the low-speed rotor, the gear ratio (2.2) is multiplied and divided, respectively. The torque-speed curve due to the mathematical method is compared in the next section.

C. Coupled Analysis

The torque-speed curve when the DC current is 40 A is computed using a transient electromagnetic field analysis under vector control (coupled analysis). The control diagram is shown in Fig. 4. The torque-speed characteristics obtained by the coupled analysis is compared with those obtained by the mathematical method in Fig. 5. From Fig. 5, the rotation speed due to the mathematical method is higher than that due to the coupled analysis. This is due to the convergence error of the d-axis current in the coupled analysis.

IV. Conclusion

This paper proposed a novel variable flux magnetic-geared motor. In order to obtain the torque-speed curve, a mathematical method and coupled analysis were conducted.

TABLE I
SPECIFICATION

Stator size	ϕ110 × 83 mm
Coil	ϕ2.1 × 10 × 1Y
DC voltage supply	12 V (3rd harmonics injection)
Material	50A1300 (Silicon steel sheet)

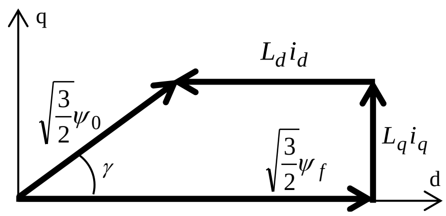

Fig. 2. Flux vector on the d-q coordinate system.

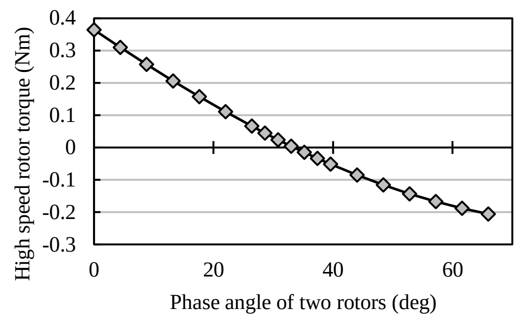

Fig. 3. Phase angle difference v.s high-speed rotor torque.

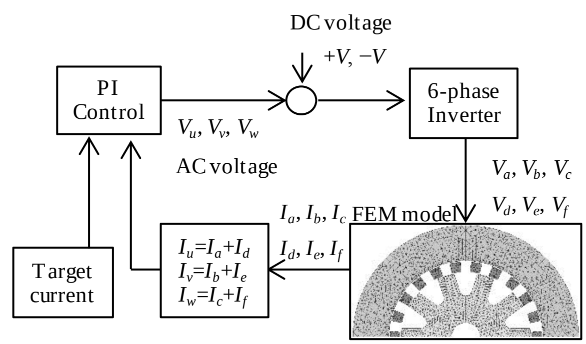

Fig. 4. Control diagram.

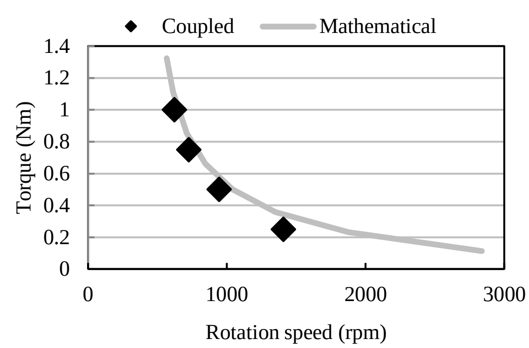

Fig. 5. Torque-rotation speed curve.

The torque-speed curve due to both methods showed a good agreement with each other. In the final paper, variable flux characteristics are discussed using the 2 methods.

References

[1] A. Kohara, K. Hirata, N. Niguchi, and Y. Ohno, "Finite-Element Analysis and Experiment of Current Superimposition Variable Flux Machine Using Permanent Magnet," *IEEE Trans. Magn.*, vol. 52, no. 9, 8107807, 2016.

[2] N. Niguchi, K. Hirata, Y. Ohno, and A. Kohara, "VARIABLE FLUX RELUCTANCE MOTOR USING A SINGLE SET OF COILS," in *Proc. XVII International Symposium on Electromagnetic Fields in Mechatronics, Electrical and ectronic Engineering*, 1A1-F-1, 2015.